Detection of heat flux at single-atom scale in a liquid-solid interfacial region based on classical molecular dynamics

K. Fujiwara, and M. Shibahara

Citation: Appl. Phys. Lett. **114**, 011601 (2019); doi: 10.1063/1.5062589
View online: https://doi.org/10.1063/1.5062589
View Table of Contents: http://aip.scitation.org/toc/apl/114/1
Published by the American Institute of Physics

Applied Physics Letters ARTICLE scitation.org/journal/apl

Detection of heat flux at single-atom scale in a liquid-solid interfacial region based on classical molecular dynamics

Cite as: Appl. Phys. Lett. **114**, 011601 (2019); doi: 10.1063/1.5062589
Submitted: 25 September 2018 · Accepted: 16 December 2018 · Published Online: 07 January 2019

K. Fujiwara[1,a)] and M. Shibahara[2]

AFFILIATIONS

[1] Center for Atomic and Molecular Technologies, Osaka University, 2-1 Yamadaoka, Suita, Osaka 565-0871, Japan
[2] Department of Mechanical Engineering, Osaka University, 2-1 Yamadaoka, Suita, Osaka 565-0871, Japan

[a)] Electronic mail: k.fujiwara@mech.eng.osaka-u.ac.jp

ABSTRACT

In this study, we examine heat flux at the single-atom scale in a liquid-solid interfacial region by calculating local quantities based on classical molecular dynamics. The heat flux was calculated over a subatomic area defined on the liquid-solid interfacial region, and a two-dimensional map of the local heat flux at the liquid-solid interface was obtained. The results clearly showed directional heat flux at the single-atom scale between the liquid and solid phases; the spatial heat conduction was not uniform along a temperature gradient in the immediate vicinity of the solid surface, which suggests that the interfacial thermal resistance can be interpreted more precisely based on the local quantity of the heat flux. The methodology and results given in this study should prove useful to more precisely interpret and control heat transfer and thermal resistance at interfaces.

It is widely known that temperature changes abruptly at the interface between different phases through which heat transfers.[1–3] The interfacial thermal resistance (ITR) R is defined using this temperature change at the interface ΔT and the heat flux j through the interface, as

$$R = \Delta T/j. \quad (1)$$

Modifying the physical and chemical properties of the interface to control the interfacial thermal resistance (ITR) is one of the central problems for thermal science and engineering,[4–6] and there has been considerable research on the evaluation of the ITR based on theory,[7–9] simulations,[10–24] and experiments.[25–30] In particular, a number of studies have been devoted to the evaluation of liquid-solid[10–17] and solid-solid[18–24] interfaces based on molecular dynamics. The physical origin behind the ITR should be pursued from a molecular perspective. However, understanding the heat transfer physics of such interfaces at the atomic scale is extremely difficult due to the complexity of the interfacial properties. Even now, it is not known precisely where the heat transfer occurs at the atomic scale, in spite of the fact that precise clarification of interfacial heat transfer is required for advances in fundamental thermal science and engineering applications.[31]

From a macroscopic point of view, the interface may be idealized as a plane without thickness; however, a microscopic picture based on the density results obtained by molecular dynamics[32] shows that the interface has a thickness of a few Å (see Fig. 1). Therefore, we believe that this interfacial region plays a crucial role in determining the characteristics of the ITR and is directly connected to the fundamental mechanisms behind the heat transfer. However, the ITR is obtained as a result of the temperature change at the interface, and Eq. (1) does not provide information on the inside of the interfacial region. As shown in Fig. 1, the interfacial region includes not only liquid phase layers in the vicinity of the solid surface but also the space between the first solid and liquid layers that directly face each other; in this region, the temperature cannot be defined due to the lack of atoms in the heat conduction direction.

However, even in such an interfacial region where the macroscopic quantity (temperature) is difficult to define, we can

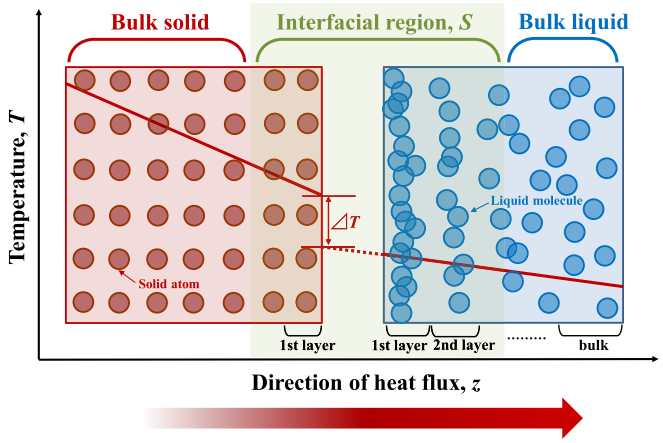

FIG. 1. Schematic illustration of a liquid-solid interface and the interfacial region at the atomic scale. In this figure, the heat flows from the solid (left) to liquid (right), and the interfacial region *S* is defined as the region between the bulk solid and liquid. There exists space between the first solid and liquid layers, where there are no atoms.

interpret the thermal resistance as a property based on the heat flux detected locally in the region, that is,

$$\mathrm{R}(x,y)|_z \propto \frac{1}{j(x,y)|_z}, \quad z \in \mathrm{S}, \tag{2}$$

where the x-y plane in the system is normal to the heat flux direction z. In Eq. (2), $\mathrm{R}(x,y)|_z$ and $j(x,y)|_z$ are the local thermal resistance and heat flux at z, respectively, which vary depending on the locations in the x-y plane, and S denotes the interfacial region in the z direction. Equation (2) indicates that the local interfacial thermal resistance (LITR) at the atomic scale is inversely proportional to the local heat flux (LHF), and it can be defined even in the region where there are no atoms as long as the local heat flux can be detected. Note that the interfacial thermal resistance $R = \Delta T/j$ in Eq. (1) is an expression for the overall ITR from a macroscopic point of view, which does not consider the quantity of local heat flux defined at the atomic scale. We propose the expression in Eq. (2) as a way to reveal local properties of the overall ITR based on the LHF. Using the LHF is a promising approach, since we can evaluate it even where the temperature is not well defined, and it is directly connected to the fundamental interpretation of the precise heat transfer phenomena in the interfacial region. Although the detection of the LHF in the interfacial region is expected to give us valuable information on interpreting the overall interfacial thermal resistance more precisely, the heat flux has not been detected locally in such an interfacial region. In the present study, we conducted non-equilibrium molecular dynamics simulations for a liquid-solid interfacial system and explored the heat flux in a liquid-solid interfacial region, which is defined locally in space and possesses atomic-scale spatial resolution. Our previous work on the elucidation of local physical quantities[33,34] enabled us to develop the techniques for obtaining the local heat flux at the single-atom scale. As a result, we have been able to develop a microscopic picture of the liquid-solid interface based on the results of the LHF.

Here, with the objective of evaluating the local heat flux in a interfacial region, we apply the microscopic expression of the heat flux for monatomic atoms, which is described as a local and instantaneous expression[13,35]

$$\mathbf{j}_e(\mathbf{r},t) = \frac{1}{\Omega_\mathbf{r}}\left[\sum_{i\in\Omega_\mathbf{r}} e_i\mathbf{v}_i + \frac{1}{2}\sum_i\sum_{j\neq i}\mathbf{r}^*_{ij}(\mathbf{v}_i\cdot\mathbf{F}_{ij})\right]. \tag{3}$$

In Eq. (3), $\Omega_\mathbf{r}$ is the local volume in the system, $\mathbf{F}$ is the force acting on the molecules, and $\mathbf{v}$ is the velocity of a particle. The total energy is defined as $e_i = (1/2)m_i\mathbf{v}_i^2 + (1/2)\Sigma_j\phi_{ij}$, where ϕ_{ij} is the potential energy between the ith and jth particles and m is the mass of a particle. The time-averaged energy flux can be obtained as $\mathbf{j}_e(\mathbf{r}) = \langle\mathbf{j}_e(\mathbf{r},t)\rangle$. Note that $\mathbf{r}^*$ is the line segment between particles in the local volume and is evaluated in the two-dimensional plane considering the effects of the three-dimensional volume in the present study. In previous work, the methodologies to obtain the local quantities have often been limited to a single dimension.[11,13,36,37] Recently, Fujiwara *et al.* obtained effects of fluctuations of the local energy fluxes in two-dimensions for evaporation processes from a vapor-liquid surface formed in a slit pore.[38] In this study, we calculated heat flux in three-dimensional space at atomic resolution in a liquid-solid interfacial region and obtained a two-dimensional map of the local heat flux by developing a technique of calculating local quantities.[33,34,36,37]

As a modelled system, we adopted a fluid sandwiched by two planar solid walls in which heat flows. The two walls were located at the lower and upper sides in the z direction of the system, and periodic boundary conditions were adopted in the x and y directions. The system size was $L_x \times L_y \times L_z = 40 \times 40 \times 39$ Å^3. Since obtaining the local heat flux requires much computational time, we adopted simple molecules and atoms: Ar molecules as the fluid and Pt atoms as the solid, whose interactions were based on van der Waals forces of the form (LJ), $\phi_{ff}(r_{ij}) = 4\varepsilon_{ff}[(\sigma_{ff}/r_{ij})^{12} - (\sigma_{ff}/r_{ij})^6]$ with a cut-off radius of 4.0 (using an Ar-Ar interaction as an example). Here, r_{ij} is the distance between the ith and jth particles, and σ_{ff} and ε_{ff} are 3.405 Å and 1.67×10^{-21} J, respectively. Hereafter, in the present study, reduced units are adopted by using the LJ parameters of Ar molecules: σ_{ff}, ε_{ff}, and mass. The reduced parameters used for the solid-solid interactions were $\sigma_{ss} = 0.746$ and $\varepsilon_{ss} = 65.39$ (Ref. 39), and the solid atoms were arranged with the fcc(111) surface facing the fluid region. The solid walls consisted of five atomic layers, and the gap between the solid walls was set to be 7.0. The temperature of the solid atoms was controlled by the Langevin method[40] at the fourth layer from the fluid region, while the outer solid atoms at the fifth layer were fixed. The LJ potential form was used also for the fluid-solid interaction, and σ_{fs} was calculated using the Lorentz-Berthelot rule. The parameter ε_{fs} was defined as a ratio to ε_{ff} and was inserted in the potential form of $\phi_{fs}(r_{ij}) = 4\varepsilon_{fs}\varepsilon_{ff}[(\sigma_{fs}/r_{ij})^{12} - (\sigma_{fs}/r_{ij})^6]$. In this study, the values of ε_{fs} were set to be 1.0 and 2.0, which constitute a wetting condition.[41] The equation of motion was integrated using the velocity Verlet method, and the simulations were conducted

with a time interval of $t^* = \sigma_{ff}(m_f/\varepsilon_{ff})^{1/2} = 9.3 \times 10^{-4}$. The initial condition was obtained as follows. First, the temperature of the fluid was maintained at 0.83 using the velocity-scaling method for 50 000 time steps, and the relaxation calculation without controlling the fluid temperature was conducted for 100 000 000 time steps. The temperatures of the upper and lower solid surfaces were set to be $T^* = \varepsilon_{ff}/k_B = 0.41$ and 1.2, respectively, by the Langevin method during the simulations, which set up a relatively large temperature gradient, with the objective of detecting the local heat flux at the single-atom scale in the liquid-solid interfacial region. Here, k_B is the Boltzmann constant. The averaged pressure ($P^* = \varepsilon_{ff}/\sigma_{ff}^3$) was 0.024 in the simulations. After the relaxation calculation, the local quantities were calculated at the resolution of $dx^* \times dz^* = 0.059 \times 0.059$ in the x–z plane, and the values obtained were averaged over 100 000 000 time steps.

First, we present the basic results obtained from the simulation which are important for the understanding of the main results to follow. Figures 2(a) and 2(b) show the one- and two-dimensional density distributions of liquid molecules in the vicinity of the lower solid surface which were calculated in the z direction and in the x-z plane, respectively. Here, the first layer of the solid atoms facing the liquid phase is located at $z^* = 0.0$. In Fig. 2(a), liquid layers are observed as shown in previous studies (for example, see Ref. 32), and the distance between the first interfacial solid and liquid layers is approximately 0.7 (≈2.4 Å). It should be stressed from the result in Fig. 2(a) that there exist no atoms or molecules between the first layers of the liquid-solid interface, and it can also be confirmed in the x-z plane in the case of $\varepsilon_{fs} = 1.0$ [Fig. 2(b)]. The result of the two-dimensional density shown in Fig. 2(b) also reveals that the liquid layers in the immediate vicinity of the solid surface are not uniform in the x^* direction. For a clear understanding, in Fig. 2(c), we present a snapshot of the configurations of solid atoms and liquid molecules in the x-z plane, which are consistent with the result shown in Fig. 2(b).

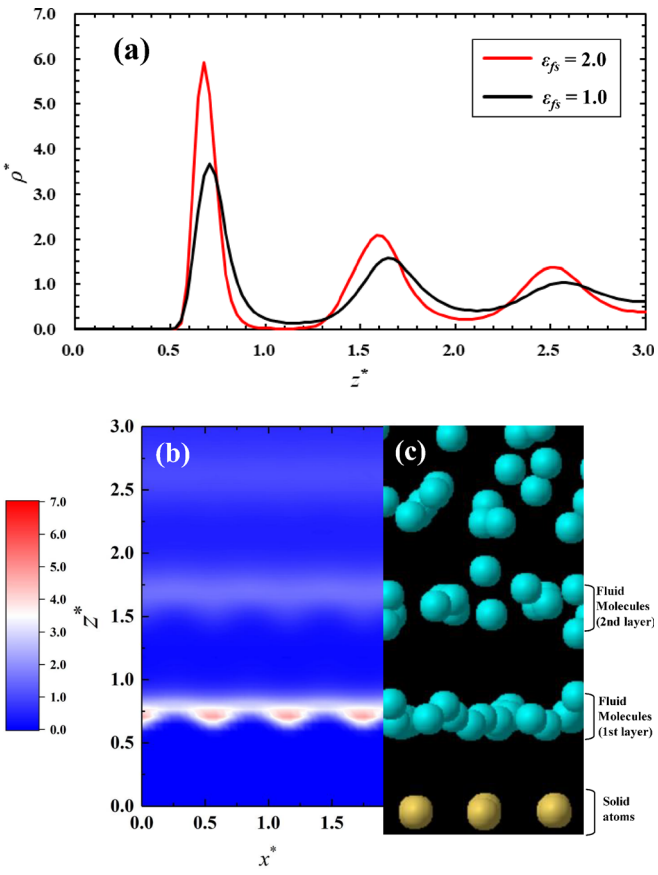

FIG. 2. Density distributions in the calculation system. (a) One-dimensional density distribution of the liquid molecules in the vicinity of the solid surface for $\varepsilon_{fs} = 1.0$ and 2.0. The results are the averaged values for 100 000 000 time steps. (b) Two-dimensional density distribution of the liquid molecules and solid atoms in the x-z plane for $\varepsilon_{fs} = 1.0$, with a snapshot of the calculation system (c). The results were obtained at a resolution of $dx^* \times dz^* = 0.059 \times 0.059$. The first layer of the solid atoms is located at $z^* = 0.0$.

The local heat fluxes were calculated based on Eq. (3) at a resolution of $dx^* \times dz^* = 0.059 \times 0.059$ which is less than a single-atom diameter and are shown in Fig. 3 as the time-averaged values during 100 000 000 time steps in the x-z plane in the cases of $\varepsilon_{fs} = 1.0$ [Fig. 3(a)] and 2.0 [Fig. 3(b)]. Figures 3(a) and 3(b) clearly reveal the directional heat fluxes in the interfacial region which includes the space between the facing first liquid and solid layers. The x^* positions of the solid atoms at $z^* = 0.0$ are 0.57, 1.14, and 1.71, respectively, which indicates that the directional heat fluxes at the atomic scale are most pronounced just above the first layer of solid atoms. It can be seen that the directional heat fluxes from the solid atoms weaken in the direction of the temperature gradient; however, the flux at the atomic scale can be detected even in the liquid layers ($z^* > 0.7$), for example, in the case of $\varepsilon_{fs} = 2.0$.

Finally, we show the values of the local heat flux obtained in the cases of $\varepsilon_{fs} = 1.0$ [Fig. 4(a)] and 2.0 [Fig. 4(b)]. As was the case in Fig. 3, high values of the local heat flux were observed in the immediate vicinity of the first solid atoms, and away from the solid surface in the direction of the temperature gradient, the heat flux becomes uniform in the x–y plane, that is, the LHF becomes consistent with the macroscopic heat flux. This observation clearly reveals that in the interfacial region, the spatial heat conduction in the z direction is not uniform in the x-z plane even in the liquid layers, and the effect was observed approximately in the range of $0.0 < z^* < 2.0$ under the present condition ($\varepsilon_{fs} = 2.0$). This result implies that the interfacial thermal resistance (ITR) can be interpreted more precisely considering the local heat flux (LHF) in the interfacial region, and the LHF gives valuable information on local properties of the overall ITR, namely, the local interfacial thermal resistance (LITR).

In this letter, we have examined the local heat flux at the single-atom scale in a liquid-solid interfacial region, developing the technique of obtaining local quantities based on molecular dynamics. In the liquid-solid interfacial region, a directional heat flux was detected which was pronounced in the immediate vicinity of the solid atoms. The effect of the local heat flux was detectable even in the liquid phase, which revealed clearly that in the interfacial region, the spatial heat conduction is not

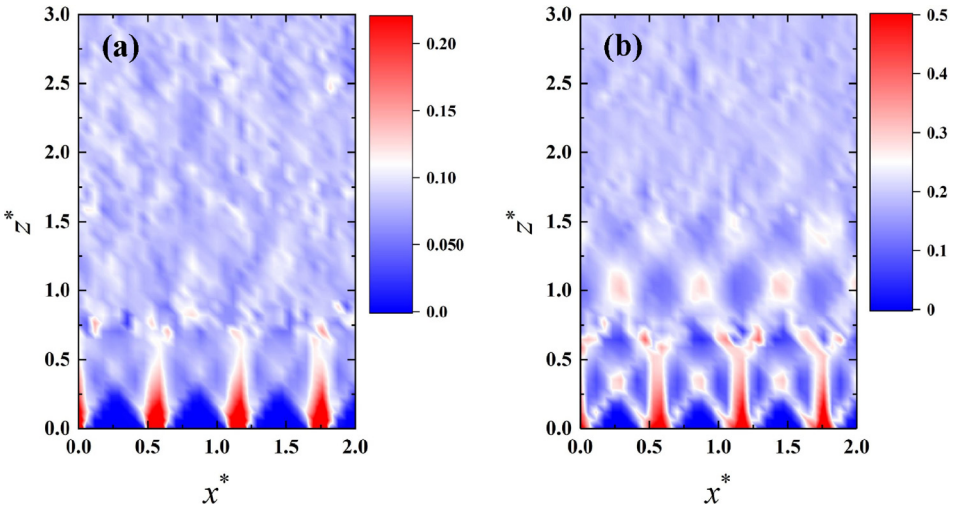

FIG. 3. Local heat flux in the liquid-solid interfacial region for $\varepsilon_{fs} =$ (a) 1.0 and (b) 2.0. The results are the averaged values for 100 000 000 time steps and obtained at a resolution of $dx^* \times dz^* = 0.059 \times 0.059$. The first layer of the solid atoms is situated at $z^* = 0.0$, and the first layer of the liquid phase exists approximately at 0.7 [see Fig. 2(b)]. The x^* positions of the three solid atoms at $z^* = 0.0$ are 0.57, 1.14, and 1.71, respectively.

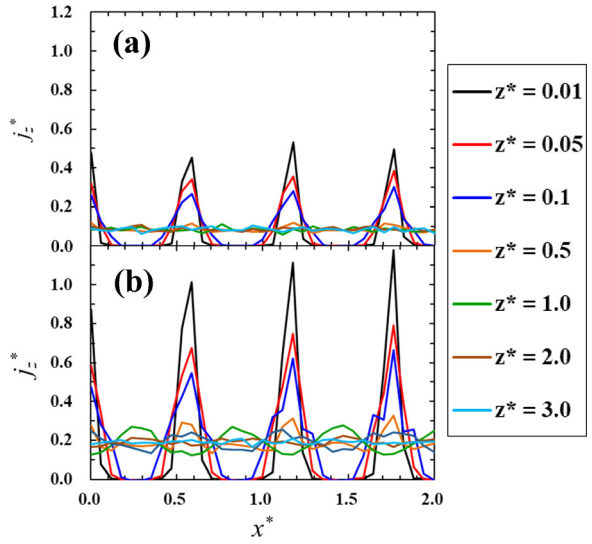

FIG. 4. Local heat flux in the liquid-solid interfacial region for various positions of z^* in the cases of $\varepsilon_{fs} =$ (a) 1.0 and (b) 2.0.

uniform at the atomic scale along the temperature gradient. The methodology and results given in this study should prove useful to more precisely interpret and control heat transfer and thermal resistance at interfaces.

This study was supported by JSPS KAKENHI Grant No. JP 17H06836.

REFERENCES

[1]P. L. Kapitza, J. Phys.(USSR) **4**, 181 (1941).
[2]R. C. Johnson and W. A. Little, Phys. Rev. **130**, 596 (1963).
[3]G. L. Pollack, Rev. Mod. Phys. **41**, 48 (1969).
[4]M. Kaviany, *Heat Transfer Physics*, 2nd ed. (Cambridge University Press, New York, 2014).
[5]D. G. Cahill, W. K. Ford, K. E. Goodson, G. D. Mahan, A. Majumdar, H. J. Maris, R. Merlin, and S. R. Phillpot, J. Appl. Phys. **93**, 793 (2003).
[6]D. G. Cahill, P. V. Braun, G. Chen, D. R. Clarke, S. Fan, K. E. Goodson, P. Keblinski, W. P. King, G. D. Mahan, A. Majumdar, H. J. Maris, S. R. Phillpot, E. Pop, and L. Shi, Appl. Phys. Rev. **1**, 011305 (2014).
[7]P. Reddy, K. Castelino, and A. Majumdar, Appl. Phys. Lett. **87**, 211908 (2005).
[8]Y. Benveniste, J. Appl. Phys. **61**, 2840 (1987).
[9]G. E. W. Bauer, K. M. Schep, K. Xia, and P. J. Kelly, J. Phys. D: Appl. Phys. **35**, 2410 (2002).
[10]L. Xue, P. Keblinski, S. R. Phillpot, S. U.-S. Choi, and J. A. Eastman, J. Chem. Phys. **118**, 337 (2003).
[11]T. Ohara and D. Torii, J. Chem. Phys. **122**, 214717 (2005).
[12]S. Murad and I. K. Puri, Appl. Phys. Lett. **92**, 133105 (2008).
[13]M. Shibahara and T. Ohara, J. Therm. Sci. Technol. **6**, 247 (2011).
[14]Y. Wang and P. Keblinski, Appl. Phys. Lett. **99**, 073112 (2011).
[15]A. T. Pham, M. Barisik, and B. Kim, Int. J. Heat Mass Transfer **97**, 422 (2016).
[16]Y. Ma, Z. Zhang, J. Chen, K. Sääskilahti, S. Volz, and J. Chen, Carbon **135**, 263 (2018).
[17]B. Cao, J. Zou, G. Hu, and G. Cao, Appl. Phys. Lett. **112**, 041603 (2018).
[18]P. K. Schelling, S. R. Phillpot, and P. Keblinski, Appl. Phys. Lett. **80**, 2484 (2002).
[19]D. Konatham and A. Striolo, Appl. Phys. Lett. **95**, 163105 (2009).
[20]E. Lampin, Q.-H. Nguyen, P. A. Francioso, and F. Cleri, Appl. Phys. Lett. **100**, 131906 (2012).
[21]J. Chen, G. Zhang, and B. Li, J. Appl. Phys. **112**, 064319 (2012).
[22]B. Deng, A. Chematynskiy, M. Khafizov, D. H. Hurley, and S. R. Phillpot, J. Appl. Phys. **115**, 084910 (2014).
[23]K. Gordiz and A. Henry, J. Appl. Phys. **121**, 025102 (2017).
[24]E. Lee and T. Luo, Appl. Phys. Lett. **112**, 011603 (2018).
[25]E. T. Swartz and R. O. Pohl, Appl. Phys. Lett. **51**, 2200 (1987).
[26]E. T. Swartz and R. O. Pohl, Rev. Mod. Phys. **61**, 605 (1989).
[27]Z. Ge, D. G. Cahill, and P. V. Braun, Phys. Rev. Lett. **96**, 186101 (2006).
[28]Z. Chen, W. Jang, W. Bao, C. N. Lau, and C. Dames, Appl. Phys. Lett. **95**, 161910 (2009).
[29]N. Yang, X. Xu, G. Zhang, and B. Li, AIP Adv. **2**, 041410 (2012).
[30]M. B. Bryning, D. E. Milkie, M. F. Islam, J. M. Kikkawa, and A. G. Yodh, Appl. Phys. Lett. **87**, 161909 (2005).
[31]A. Shahzad, M.-G. He, S. I. Haider, and Y. Feng, Phys. Plasma **24**, 093701 (2017).
[32]G. J. Wang and N. G. Hadjiconstantinou, Phys. Rev. Fluids **2**, 094201 (2017).

[33]K. Fujiwara and M. Shibahara, J. Chem. Phys. **141**, 034707 (2014).
[34]K. Fujiwara and M. Shibahara, J. Chem. Phys. **142**, 094702 (2015).
[35]T. Ohara, J. Chem. Phys. **111**, 9667 (1999).
[36]A. Ghoufi, F. Goujon, V. Lachet, and P. Malfreyt, Phys. Rev. E **77**, 031601 (2008).
[37]A. Ghoufi and P. Malfreyt, J. Chem. Phys. **135**, 104105 (2011).
[38]K. Fujiwara and M. Shibahara, AIP Adv. **8**, 025124 (2018).
[39]S. Zhu and M. R. Philpott, J. Chem. Phys. **100**, 6961 (1994).
[40]J. C. Tully, J. Chem. Phys. **73**, 1975 (1980).
[41]B. Shi and V. K. Dhir, J. Chem. Phys. **130**, 034705 (2009).